Journal of Engineering Mathematics, Vol. 14, No. 3, July 1980

The influence of nonparallelism in channel flow stability

P. M. EAGLES

Mathematics Department, The City University, London E.C.1, England

and

F. T. SMITH

Mathematics Department, Imperial College, London S.W.7, England.

(Received November 30, 1979)

SUMMARY

Considered below are the high Reynolds number flows of an incompressible fluid, and their nonparallel stability properties, in certain plane channels whose widths vary slowly in the streamwise direction. The first approximation to the steady-state flow is governed by the classical boundary layer equations but with the pressure unknown. Solutions, some including separation and reattachment, to this are obtained numerically for a range of the parameters involved, and the stability of the resulting flows is considered using fixed frequency disturbances and taking into account the nonparallel nature of the basic flow by use of a W.K.B. method. The calculations yield critical Reynolds numbers, below which all the disturbances decay downstream, and for various Reynolds numbers above the critical values the growths of the small disturbances are calculated. The results are specialized to a particular class of channels which are straight far upstream and far downstream but vary in between. So the predictions should be much more easily amenable to experimental investigation and comparisons than those of the more idealized, diverging channel, flow problem studied by Eagles & Weissman [1] and the only other basic flow seriously studied from the viewpoint of nonparallel flow stability theory, the Blasius boundary layer. The results also represent the first application of both quasi-parallel and slightly non-parallel stability theory to channels involving slowly varying but finite changes in width.

1. Introduction

The linear stability of slightly nonparallel flows is a very complicated matter and its application to internal or external streaming flows, in channels and boundary layers, has recently received considerable theoretical attention. The main aim of the theoretical treatments is to obtain some measure of improvement upon the quasi-parallel theory, which had previously been used extensively but without much knowledge of its limitations. For external flows, Bouthier [2], [3], Gaster [4] & Smith [5] have considered the theoretical nonparallel flow stability of the Blasius boundary layer on a flat plate. For internal flows Eagles & Weissman [1] have examined the nonparallel stability of the flow in a straight-walled divergent channel, with a small divergence angle proportional to the inverse of the Reynolds number. All these papers studied fixed frequency disturbances of the basic flow, incidentally, and attempted a determination of their growth or decay with increasing distance downstream. Other theoretical contributions have been made by Ling & Reynolds [6], Drazin [7] and Nayfeh, Mook & Saric [8]. Some experimental investigations have also been made on the stability of nonparallel flows but mainly for

external boundary layers (e.g., Schubauer & Skramstad [9], Ross, Barnes, Burns & Ross [10]).

Related experimental work on the stability properties of slightly nonparallel flows through channels, which is the concern of this paper, appears to be virtually non-existent, however. Probably one of the main difficulties in attempting an experimental verification of the theoretical predictions of Eagles & Weissman [1], the only previous study of internal nonparallel flow stability, is that of setting up the original Jeffery-Hamel steady flows they considered. For if we curve the channel walls from parallel to divergent, in order to produce a straight-walled divergent section of channel, in practice there is no simple analytic theory available which describes the effect of the curvature, even in the steady state. It is true that Fraenkel's [11], [12] internal flow theory of the effects of very small wall curvatures may be used to describe flows whose first approximations are everywhere Jeffery-Hamel flows, but in the case considered by Eagles & Weissman [1] of high Reynolds number and small angle of divergence, with the product of the Reynolds number and the divergence angle remaining of order unity, the length and ultimate width of channel required in practice would be 'enormous', to quote Fraenkel, and so of doubtful value experimentally. Even then, the effect of wall curvature on stability would be rather difficult to predict, though almost certainly of smaller order of magnitude than the effects described by Eagles & Weissman [1]. Severe difficulties, then, would be encountered experimentally in any attempt to compare with the theoretical predictions of Eagles & Weissman [1].

To partly remedy these difficulties in relation to experimental verification of nonparallel channel flow stability we will consider theoretically the following flow problem, which we believe presents a much more realizable flow situation physically. Let x, y be dimensionless rectangular Cartesian co-ordinates and let the slowly varying walls of the channel be given by $y = \pm H(X)$, where $X = \epsilon x$ is a 'slow variable' and ϵ is small. This is not the case considered by Fraenkel [11, 12], incidentally; his case is considerably more involved. Let R be the characteristic Reynolds number based on half the volumetric flow rate and defined precisely in (2.2) below, and set $R\epsilon = \lambda$. Clearly if $\lambda \ll 1$ (as $\epsilon \to 0$) then a steady state flow theory may be developed in which Poiseuille flow forms a valid first approximation. A more interesting case, the one we study here, is to take λ to be constant, i.e. independent of ϵ in the limit as $\epsilon \to 0$ and $R \to \infty$. Then a stream function of the form $\psi = \Psi(X,y)$ yields a first approximation which satisfies the nonlinear boundary layer equation, and so the steady state flow deviates nonlinearly from Poiseuille flow and includes the possibility of separation and reattachment taking place. Such a possibility would be expected to have a dramatic effect on the stability properties of the motion.

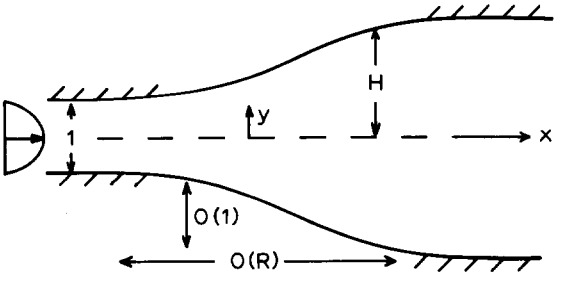

Figure 1. The non-dimensional geometry of the channel and the coordinates used.

In fact we specialize in this paper to the case of the expanding channel with walls given by $H(X) = 1 + \frac{1}{2}\tanh X$. So $H(-\infty) = \frac{1}{2}$, $H(\infty) = 3/2$ and the flow far upstream and far downstream is expected to be plane parallel Poiseuille flow. The steady nonparallel flow in between is found numerically (see Sec. 2) including some cases with separation and reattachment which, here, are regular phenomena. Indeed, our solutions are almost certainly the simplest examples yet found of boundary layer flows admitting regular separation and reattachment. Equally significantly, they provide a uniformly valid leading order description of the entire flow field, a most unusual but highly desirable attribute in a separating flow at high Reynolds number. The linear nonparallel and parallel stability of the channel flows is then studied using fixed frequency disturbances. The theoretical method is described in Sec. 3, the calculation method and results are presented in Sec. 4, and a final discussion is given in Sec. 5. In contrast to the only cases of nonparallel flows studied previously for nonparallel effects, e.g. the straight-walled channel (Eagles & Weissman [1]) and the boundary layer (Bouthier [2, 3], Gaster [4], Smith [5]), there is no simple similarity solution for the steady state flows in our cases and so the form of the basic flow is different at each X-station and for each given value of λ. Further the results obtained represent, to the best of our knowledge, the first application of even quasi-parallel stability theory to channels having slowly varying but finite changes in width. We believe that the results should be much more useful practically and much more readily amenable to experimental study.

The main predictions are summarized in Figure 4 below where we show a graph of two critical Reynolds numbers versus λ. The continuous curve in Figure 4 is that based on the nonparallel theory using as the representative disturbance quantity the growth rate of the kinetic energy density of the disturbances, while the dashed curve is based on quasi-parallel stability theory. In using this figure one should recall that the relation $R\epsilon = \lambda$ holds and that the channel walls are given by $y = \pm(1 + \frac{1}{2}\tanh \epsilon x)$. Thus for a given channel of this form and a given Reynolds number we may calculate the value of λ; then if the point (R, λ) is to the left of the continuous curve the flow is completely stable to the fixed frequency disturbances considered in this paper and to any superposition of these. On the other hand, if the point (R, λ) is to the right of the curve then some fixed frequency disturbances will grow downstream over a limited range of values of X, so the flow is unstable in this sense. We also plot the stable and unstable regions in the ϵ, R plane in Figure 5 and present a further discussion and the interpretation of all the results in Sec. 5.

Our emphasis, then, is on producing theoretical predictions of the stability properties in certain reasonable, nonparallel, channel flow situations with the hope that experimental comparisons may be made. We believe it is likely that a general random small disturbance may be regarded as containing, by fourier decomposition, components of the fixed frequency type considered here. So in principle experiments could be performed to examine what practical evidence there is of instability in the regions predicted by the present theory. The work here also enables us to quantify to some extent the differences between quasi-parallel and nonparallel stability theory. The differences do not turn out to be especially excessive, at least in terms of the predictions for the critical Reynolds numbers for instance.

2. The steady state flow

Our concern in this section is with the steady planar laminar flow at high Reynolds number through a fixed channel of slowly varying shape. Far upstream the channel walls are taken to be parallel and to contain incompressible fluid in plane Poiseuille motion. We let ψ, (u, v), p denote the stream function, the velocity vector and the fluid pressure, nondimensionalized with respect to M, M/a and $\rho M^2/a^2$ respectively, where $2M$, a,ρ are in turn the volumetric flow rate per unit thickness of the oncoming Poiseuille flow, the undisturbed channel width and the fluid density. The oncoming flow is then described by

$$\psi \to 3y - 4y^3, \quad u \to 3 - 12y^2, \quad v \to 0, \quad \frac{\partial p}{\partial x} \to \frac{-24}{R} \quad \text{as } x \to -\infty. \tag{2.1}$$

Here x, y are rectangular Cartesian co-ordinates in the streamwise and transverse directions respectively, nondimensionalized with respect to a. Thus the channel walls far upstream are given by $y = \pm\frac{1}{2}$. Also, R is the Reynolds number defined by

$$R = M/\nu. \tag{2.2}$$

A more usual Reynolds number might be defined as

$$\hat{R}(X) = U_0(X)aH(X)/\nu$$

where U_0 is the streamwise velocity at the centre of the channel. But then $\hat{R}(X)$ varies with X; so the absolute definition (2.2) is more suitable. It may be easily shown that

$$\hat{R}(\pm\infty) = (3/2)R$$

however.

The equations governing ψ, u, v and p in general are the Navier-Stokes equations, while the boundary conditions supplementing (2.1) are the no-slip conditions at the walls and a downstream condition of boundedness as $x \to \infty$, although the latter need not concern us in detail here. The nondimensionalization is chosen to ensure that $\psi = \pm 1$ on the upper and lower walls respectively.

Turning now to the choice made for the degree of slow variation of the channel walls, we decide to study a channel whose typical axial length scale is $O(R)$, i.e. the slopes of the channel walls are $O(R^{-1})$ typically. The two main reasons for this choice are, first, that longer typical axial length scales generally produce a basic flow which is essentially just a minor perturbation of the original Poiseuille flow (e.g. Wilson [13], Tutty [14]), while, second, shorter length scales tend to lead to multi-structured flow fields (Smith [15, 16, 17]), often involving separation and detached shear layers. The overall properties of the latter flowfields are much too complicated to permit a convincing stability analysis to follow readily. By contrast, with our choice of typical length scale the slowly varying flow field is single-structured, it is governed by the classical boundary layer equations throughout and yet it is fully nonlinear, implying that such

interesting effects as inflexion points in the velocity profiles and even separation and reattachment can arise.

Suppose then that the channel width $2H$ is a function of the slow streamwise co-ordinate X, where

$$X = \epsilon x \tag{2.3}$$

and ϵ is the small parameter described in the introduction. Thus in accordance with the above discussion we suppose also that R and ϵ are related in the form

$$R\epsilon = \lambda \tag{2.4}$$

where λ is an $O(1)$ constant, the channel shape factor. We shall later vary λ and so obtain a number of different flow fields. It is natural to suppose that ψ is a function of X and y and then we find that a consistent asymptotic expansion of the flow solution can be made in the form

$$\psi = \Psi(X,y) + O(\epsilon^2) \tag{2.5}$$

The associated velocities and pressure expand in the form

$$u = U(X,y) + O(\epsilon^2), \quad v = \epsilon V(X,y) + O(\epsilon^3), \quad p = P(X) + O(\epsilon^2) \tag{2.6}$$

and so the lowest order streamwise momentum equation reduces to the boundary layer equation

$$UU_X - \Psi_X U_y = -dP/dX + U_{yy}/\lambda, \quad \text{with } U = \Psi_y. \tag{2.7a}$$

The boundary conditions on (2.7a) are

$$\Psi(-\infty,y) = 3y - 4y^3, \quad U(-\infty,y) = 3 - 12y^2,$$
$$\frac{dP}{dX}(-\infty) = -24\lambda^{-1}, \tag{2.7b}$$

$$\Psi = -1, \quad U = 0 \quad \text{at} \quad y = S(X) - H(X),$$
$$\Psi = \quad 1, \quad U = 0 \quad \text{at} \quad y = S(X) + H(X). \tag{2.7c}$$

Here $y = S(X)$ denotes the centre line of the channel. Also, equation (2.7b) matches with the oncoming flow properties (2.1), and (2.7c) ensures no slip at the walls as well as constant flux. It is noteworthy that the influence of $S(X)$ in (2.7a-c) can be extracted by using the co-ordinate $y - S(X)$ in place of y (this is the Prandtl transformation), so that without loss of generality we put $S(X) = 0$ henceforth. Again, the pressure $P(X)$ in (2.7a) is unknown, to be found as we proceed with the flow calculation, and therefore any separation, if it occurs, is almost certain to

be a regular phenomenon, without the spurious Goldstein [18] singularity which would be forced by having a prescribed pressure distribution instead, such as can arise in an outer or inviscid region of an external flow. Finally, a symmetry condition, $\Psi = 0 = U_y$ at $y = S(X)$ may be assumed in place of the conditions at one of the walls, if desired.

The solution to (2.7a-c) can be obtained in principle by marching forward from the incoming solution, since the governing boundary layer equation (2.7a) is locally parabolic in the X-direction, provided there is no flow reversal (see below). In general a solution by numerical means is most desirable, for although some further simplification can be effected by taking $H(X) = bX$ (b = constant) to obtain a limiting class of Jeffery-Hamel flows (Fraenkel [11], [12]) the connection with physically realisable flows is far from obvious.

To treat (2.7a-c) numerically we first transform the y-co-ordinate to make the walls become co-ordinate lines. Thus we set

$$\eta = y/H(X), \quad \text{and} \quad \Psi = F(X,\eta), \tag{2.8a}$$

yielding the governing equation and boundary conditions

$$F_{\eta\eta\eta} + \lambda \left[H(F_{\eta\eta}F_X - F_\eta F_{\eta X}) + \frac{dH}{dX} F_\eta^2 \right] - \lambda H^3 \frac{dP}{dX} = 0, \tag{2.9a}$$

$$F(X,\pm 1) = \pm 1, \quad F_\eta(X,\pm 1) = 0, \tag{2.9b}$$

$$F(-\infty,\eta) = \tfrac{3}{2}\eta - \tfrac{1}{2}\eta^3, \tag{2.9c}$$

$$dP/dX(-\infty) = -24\lambda^{-1}$$

in place of (2.7a-c). We note in passing that (2.9a) is the integral with respect to η of the vorticity equation

$$F_{\eta\eta\eta\eta} + 2\lambda \frac{dH}{dX} F_\eta F_{\eta\eta} + \lambda H(X)(F_{\eta\eta\eta}F_X - F_\eta F_{\eta\eta X}) = 0. \tag{2.10}$$

From this we can see that if dH/dX is constant then solutions independent of X are allowable: these are precisely the Jeffery-Hamel solutions mentioned earlier.

In the computational approach the equation (2.9a) was replaced by three first order central difference equations in the variables F, s, T and P where $s = F_\eta$ and $T = s_\eta$ (as in Keller & Cebeci [19], Smith [20]). The difference equations along with (2.9b) were then solved step by step in the X-direction, starting from the incoming Poiseuille flow profiles $F = (3\eta - \eta^3)/2$, $s = 3(1 - \eta^2)/2$, $T = -3\eta$ set at an initial upstream station $X = X_{-\infty}$. Uniform steps ΔX were taken, the nonlinear equations being solved at each step by Newton iteration incorporating a modified Gaussian elimination process.

The channels considered were described by the wall shapes

$$H(X) = 1 + \tfrac{1}{2}\tanh X \tag{2.11}$$

for various values of λ (= $R\epsilon$). The calculations outlined above were marched forward until the new Poiseuille flow appropriate to the wider uniform channel ($y = \pm 3/2$) far downstream was almost achieved. Tests carried out on the numerical scheme suggested that a grid with $\Delta X = 0.01$, $\Delta\eta = 0.01$, $X_{-\infty} = -4.5$ and an iterative tolerance of 10^{-7} were sufficient for an accuracy of about 0.0001 in P and τ, where τ is the scaled skin friction $\partial U/\partial y$ evaluated at $\eta = -1$.

Other tests on the computer program were made as follows. Firstly $H(X)$ was chosen to be X, so that a Jeffery-Hamel profile independent of X is a solution. Starting with the appropriate Jeffery-Hamel profile, this was found to be maintained by marching forward. Secondly, channels were taken with straight-walled portions separated by curved portions (with H and H' kept continuous). Starting from a Jeffery-Hamel profile the solution was marched forward along a straight-walled section, through a curved section, and then continued into another straight-

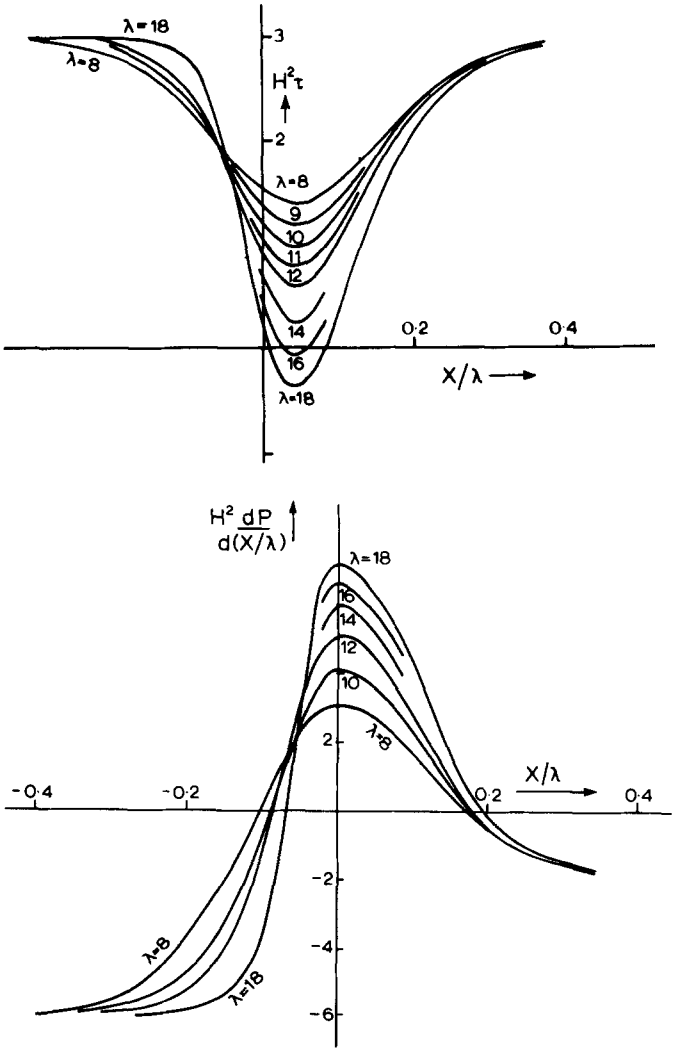

Figure 2. The skin friction and pressure gradient for the basic flows. Graphs of (a) $H^2\tau$ (= $F_{\eta\eta}$ at $\eta = -1$) and (b) $H^2 dP/d(X/\lambda)$ against X/λ for the various values of λ shown.

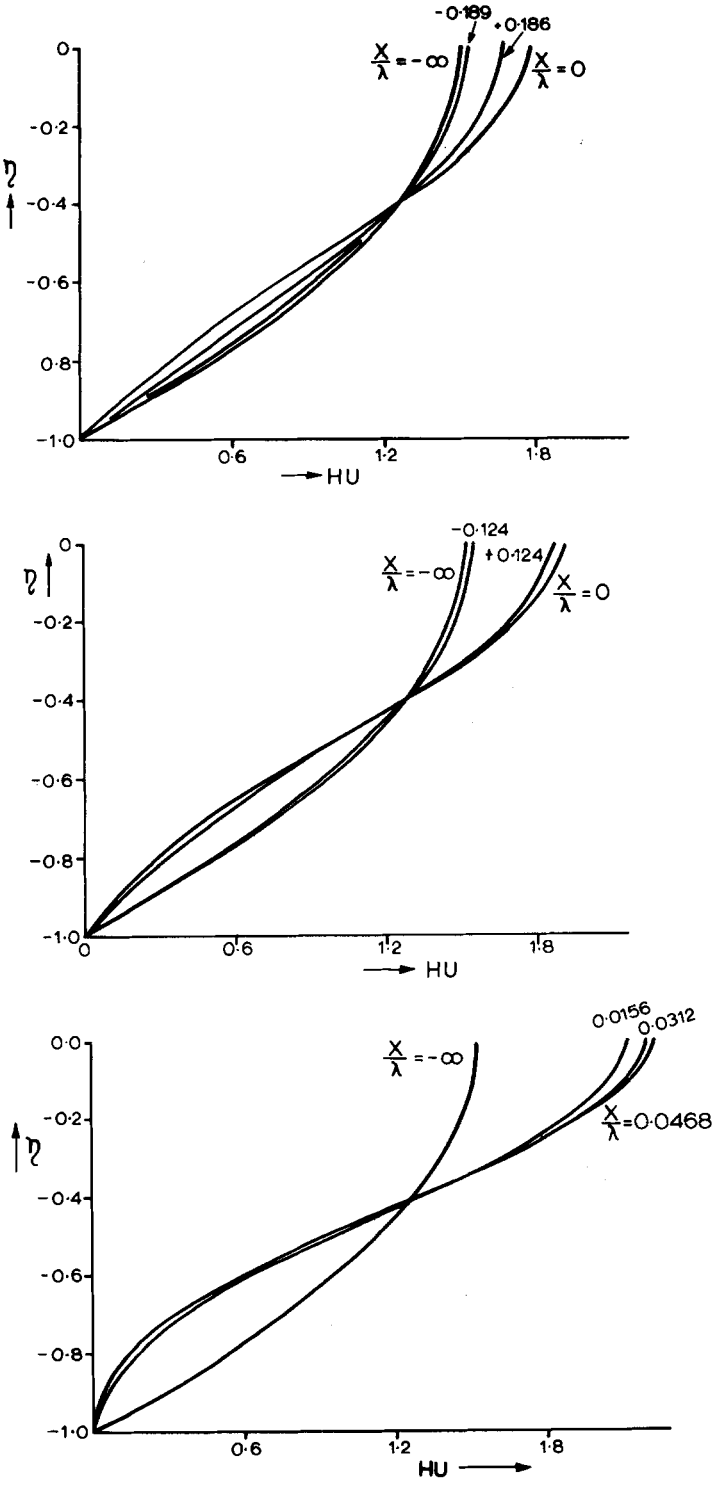

Figure 3. Some sample velocity profiles of the basic flows. Solutions for HU (= F_η) versus η for (a) $\lambda = 8$, (b) $\lambda = 12$, (c) $\lambda = 16$, at the X values shown.

walled section. The appropriate Jeffery-Hamel profile was almost exactly attained at values of X typically about 5.0 past the beginning of the second straight-walled section.

Reverting now to the expanding channel given by (2.11) we show the numerical solutions for the skin friction τ and the pressure P against X, for various values of λ, in Figure 2. The trend observed there is for the deviation from the incoming form in (2.9c) to occur fairly swiftly on the present X scale [of course physically the variation is slow], with the pressure gradient dP/dX rising and the skin friction τ falling through the mouth of the channel (around $X = 0$). Then τ reaches a minimum, dP/dX a maximum and thereafter the flow slowly attains the ultimate downstream Poiseuille form. As λ increases the severity of the channel expansion increases and, in accordance, the minimum value of τ falls, until regular separation ($\tau = 0$) is just achieved for $\lambda \doteqdot 15.5$ at $X \doteqdot 0.35$. The solutions with $\lambda = 16, 18$ exhibit regions of flow reversal wherein $\tau < 0$. These were computed using the forward marching scheme, incidentally, an approach which might be thought invalid/unstable numerically but which nevertheless is known to produce accurate solutions throughout the flow field provided that, as here, the reversed flow is not excessive. Typical samples of the velocity profiles are presented in Figure 3. It is noticeable both in Figure 2 and Figure 3 that as λ is increased the upstream influence of the channel deviation decreases while the downstream influence increases, along with the rise in the maximum pressure gradient.

Given the above solutions for the basic steady state flows we move on to consider next (Secs. 3, 4) their stability, making use of their slowly varying character.

3. Nonparallel flow stability of fixed frequency disturbances

The basic steady-state stream function studied in §2 may be written $\psi = F(X,\eta) + O(\epsilon^2)$ from (2.5) and (2.8b), where $\eta = y/H(X)$. It follows that the partial differential equation for a linear disturbance to the basic flow has coefficients independent of time. Hence we are able to consider linear disturbances with fixed frequency. Specifically we set $\psi = F(X, \eta) + O(\epsilon^2) + f(X, \eta, t)$ where the stream function f of the disturbance is expressed in the form

$$f(X,\eta,t) = e^{-i\omega t + iS}[f_0(X,\eta) + \epsilon f_1(X,\eta) + \ldots] + c.c. . \tag{3.1}$$

Here c.c. denotes the complex conjugate of the preceding expression, and we must allow S to vary slowly in the streamwise direction since the basic flow does. Thus we have

$$\frac{dS}{dx} = Q(X), \tag{3.2}$$

say, to allow for the slowly varying coefficients in the governing partial differential equation of the disturbance. We choose ω in (3.1) to be real. This is effectively the W.K.B. modification of the simple linear disturbance $e^{-i\omega t + ikx} f(y)$ which would be used in strictly parallel flow, or in a quasi-parallel approximation. The time t here is nondimensionalized with respect to a^2/M.

There is one theoretical point to discuss here before we proceed to the details of the expansion. We shall substitute ψ into the full vorticity equation

$$\left[\frac{\partial}{\partial t}+\frac{\partial\psi}{\partial y}\frac{\partial}{\partial x}-\frac{\partial\psi}{\partial x}\frac{\partial}{\partial y}\right]\nabla^2\psi=\frac{1}{R}\nabla^4\psi,$$

linearize in f and treat the Reynolds number R as being independent of the small parameter ϵ in the asymptotic expansion of the disturbance. This method is virtually the same as the approach adopted by Bouthier [2], [3], Gaster [4] and Eagles & Weissman [1]. It is believed to be both accurate and desirable, in this problem, to adopt the above method and then to return to the relation $R\epsilon = \lambda$ when we apply and interpret the results. Fairly extensive numerically based arguments in support of the approach are given in the papers cited above. An alternative analytically based approach is to retain the relation $R = \lambda/\epsilon$ throughout, which leads to a singular perturbation analysis of some complexity. This approach has been adopted by Smith [5], and applied to the lower branch properties of the neutral curve for boundary layer stability. His results are in fairly good agreement numerically with those of Bouthier and Gaster, however. The present method is also supported by the results of a numerical attack on the full partial differential equation for the small fixed frequency disturbance to a Jeffery-Hamel flow. The results of this study, by Allmen [21], are in close agreement with the results of Eagles & Weissman [1]. Thus some confidence seems justified in the present method.

We proceed now with the expansion. On substituting ψ into (3.3) we find that the leading order disturbance f_0 satisfies the equation

$$\mathscr{L}(f_0)=0$$

where the operator $\mathscr{L}$ is defined by

$$\mathscr{L}\equiv[R^{-1}(D^2-K^2)^2-iK\{(F_\eta-\beta/K)(D^2-K^2)-F_{\eta\eta\eta}\}],\quad D\equiv\partial/\partial\eta, \tag{3.4}$$

and

$$K(X)=Q(X)H(X),\quad \beta(X)=\omega H^2(X). \tag{3.5a,b}$$

The boundary conditions on $f_0(X,\eta)$ are

$$f_{0\eta}=f_{0\eta\eta\eta}=0 \quad \text{at} \quad \eta=0,\quad f_0=f_{0\eta}=0 \quad \text{at} \quad \eta=1, \tag{3.6}$$

for a symmetric disturbance which is well known to be the most unstable and therefore most worthy of study. The functions $K(X)$ and $\beta(X)$ in (3.5a, b) may be termed the local wave number and frequency, these being the values of the wave number and frequency nondimensionalized by the local length scale $aH(X)$. However, it must be emphasised that, whereas ω is kept constant as required by the governing equation for the disturbance, the local frequency β varies with X.

Equation (3.4) and its boundary conditions (3.6) constitute the 'local' Orr-Sommerfeld problem and yield the results of a parallel flow approximation. Given ω (real) we may solve for the complex value of $K(X)$ and for the complex eigenfunction $f_0(X, \eta)$ at each X station. In fact it is convenient to set

$$f_0(X,\eta)=A(X)g_0(X,\eta) \tag{3.7}$$

where g_0 is normalized in some definite manner, but where the complex amplitude function $A(X)$ is unknown at the present stage. In the numerical calculations described later we took $g_0(X, 0) = 1$ as the normalization.

At the next order in the expansion the equation satisfied by f_1 is found to be

$$\mathscr{L}(f_1) = \frac{dA}{dX}(g_0 B_1 + g_{0\eta\eta} B_2) + A(X)(g_{0X} B_1 + g_{0\eta\eta X} B_2 + B_3) \tag{3.8a}$$

where B_1, B_2, B_3 and g_0 are known functions of X and η. Explicitly we have after some manipulation

$$B_1 = 2\omega H^4 Q - 3H^3 Q^2 F_\eta - HF_{\eta\eta\eta} + 4iH^4 Q^3/R, \tag{3.8b}$$

$$B_2 = HF_\eta - 4iH^2 Q/R, \tag{3.8c}$$

$$\begin{aligned} B_3 = {} & g_0 \left(\omega H^4 \frac{dQ}{dX} - 3H^3 Q \frac{dQ}{dX} F_\eta + \frac{6iH^4 Q^2}{R} \frac{dQ}{dX} \right) + g_{0\eta} \\ & \left(-2H^3 \omega Q \frac{dH}{dX} \eta + 2H^2 \frac{dH}{dX} Q^2 \eta F_\eta \right. \\ & \left. - 2 \frac{dH}{dX} F_{\eta\eta} + H^3 Q^2 F_X + HF_{\eta\eta X} - \frac{4iH^3}{R} \frac{dH}{dX} Q^3 \eta \right) \\ & + g_{0\eta\eta} \left(-2 \frac{dH}{dX} F_\eta + \frac{8iH}{R} \frac{dH}{dX} Q - \frac{2iH^2}{R} \frac{dQ}{dX} \right) + g_{0\eta\eta\eta} \left(-HF_X + \frac{4iH}{R} \frac{dH}{dX} Q\eta \right. \end{aligned} \tag{3.8d}$$

We observe that these expressions for B_1, B_2, B_3 depend only on first order derivatives with respect to X, but up to third order derivatives with respect to η, of the known steady state stream function $F(X,\eta)$ determined in Sec. 2, as well as on the known eigenfunctions $g_0(X,\eta)$, on $Q(X)$ and on the channel semi-width $H(X)$.

The boundary conditions on f_1 are exactly the same as those on f_0, of course, and therefore (3.8) has a solution if and only if the correct orthogonality (or compatability) condition is satisfied. In the usual way (c.f. Stuart [22], Watson [23]) if the adjoint eigenfunction $v(X, \eta)$ is defined by the governing equation and boundary conditions

$$\begin{aligned} & \frac{1}{R}(D^2 - K^2)^2 v = iK \left[\left(F_\eta - \frac{\beta}{K} \right) (D^2 - K^2) v + 2F_{\eta\eta} Dv \right], \\ & v = Dv = 0 \quad \text{at} \quad \eta = 1, \\ & Dv = D^3 v = 0 \quad \text{at} \quad \eta = 0, \end{aligned} \tag{3.9}$$

then the required orthogonality condition is that the integral with respect to η, from 0 to 1, of the product of v with the righthand side of (3.8a) is zero. This yields the ordinary differential equation

$$H_1(X)A + H_2(X)\frac{dA}{dX} = 0 \tag{3.10}$$

for the amplitude function $A(X)$ of (3.7), where H_1, H_2 are now known functions specified by

$$H_1(X) = \int_0^1 \nu g_{0X} B_1 d\eta + \int_0^1 \nu g_{0\eta\eta X} B_2 d\eta + \int_0^1 \nu B_3 d\eta, \tag{3.11}$$

$$H_2(X) = \int_0^1 \nu g_0 B_1 d\eta + \int_0^1 \nu g_{0\eta\eta} B_2 d\eta. \tag{3.12}$$

To summarize, then, we may specify ω and R, solve (3.4) – (3.6) for f_0 and $K(X)$ and then normalize to obtain g_0 [in (3.7)]; solve (3.9) for ν, and use (3.10) to obtain $dA(X)/dX$.

We are interested next in the growth or decay of these disturbances as the downstream distance increases. As explained by Eagles & Weissman [1] and earlier by Gaster [4] the growth rate depends on the particular physical quantity chosen for examination. Here we concentrate on a general measure of the disturbance, its kinetic energy density, defined by

$$E(X) = \frac{\rho}{2} \int_0^{H(X)} \int_0^{2\pi/\omega} \{(u')^2 + (v')^2\} dt\, dy \tag{3.13}$$

where u' and v' are the velocity components of the disturbance.
The expressions for u' and v' are

$$u' = \frac{1}{H} e^{-i\omega t + iS} \left\{ A(X) \frac{\partial g_0}{\partial \eta} + O(\epsilon) \right\} + \text{c.c.} \tag{3.14}$$

$$v' = -e^{-i\omega t + iS} \{ iQ(X)A(X)g_0 + O(\epsilon) \} + \text{c.c.} \tag{3.15}$$

where c.c. denotes the complex conjugate of the preceding expression and we find

$$E(X) = |A|^2 \frac{\rho}{2} \exp(-2S_i) \int_0^1 \left\{ \frac{|g_{0\eta}|^2}{H^2} + |Q|^2 |g_0|^2 \right\} H\, d\eta + O(\epsilon) \tag{3.16}$$

where S_i denotes the imaginary part of $S(X)$. Defining

$$M(X) = \int_0^1 \left\{ \frac{|g_{0\eta}|^2}{H} + H|Qg_0|^2 \right\} d\eta \tag{3.17}$$

we find the growth rate associated with the energy is

$$G_E(X) \equiv E^{-1} dE/dx = \frac{-2K_i(X)}{H(X)} + \epsilon \left\{ \frac{2d|A|/dX}{|A|} + \frac{dM/dX}{M} \right\} + O(\epsilon^2) \tag{3.18}$$

where we have used the relation $dS/dx = Q(X) = K(X)/H(X)$ stemming from (3.2), (3.5a) and borne in mind that the derivative with respect to x of the $O(\epsilon)$ term in (3.16) is only $O(\epsilon^2)$. In comparing this with the growth rates in the Eagles & Weissman [1] work, in which the leading term is $-K_i(X)$, one must remember that the growth rates in [1] are evaluated with respect to a different quantity and to a different coordinate. Thus in (x, y) space the growth rates of [1] *do* have leading term $-K_i$ divided by the channel half-width, where $K(X)$ is the eigenvalue of the local Orr-Sommerfeld problem. Likewise, the factor of 2 in (3.18) occurs simply because of a different definition used here.

In principle, then, we may calculate the growth rate for any given values of the parameters R, λ, ω and the coordinate X. The results are expected to be valid for sufficiently small values of ϵ; and in applying them we must return to the relation $R\epsilon = \lambda$.

4. Stability calculations and results

We turn now to the computational tasks necessary to produce predictions from the stability theory of Sec. 3. For computational purposes, it proved convenient to first fix the value of λ in (2.4), and then calculate the steady-state stream function $F(X, \eta;\lambda)$ as described in Sec. 2; after that a search was conducted to find that value of R (at particular fixed values of λ, X) which divides the regime where some fixed frequency waves grow downstream from the regime where all fixed frequency waves decay downstream i.e. we searched for what may be termed $R_{\text{crit}}(\lambda, X)$.

The strategy adopted was first to calculate the growth rate for three values of the frequency ω at a given Reynolds number R; then to interpolate to that value of ω which gave the minimum growth rate for that value of R; to repeat with two other values of R and interpolate (or if necessary extrapolate) to a point (R,ω) in R-ω space where the minimum growth rate was zero. New starting values were then chosen and the process above was repeated until the critical point $(R_{\text{crit}}, \omega_{\text{crit}})$ in R-ω space, for the given station X and channel shape factor λ, was found with sufficient accuracy.

This process was completed for a range of values of λ and X and some of the results thus obtained are presented in Table 1, both for (i) the value of R_{crit} based on the energy density (see Sec. 3) and for (ii) that based only on the growth rate $-Q_i(X)$, i.e. the quasi-parallel growth rate.

Next we interpolated over the range of values of X, for each λ, to find the minimum value of R_{crit} (λ, X) for each λ, which we may call $R^*_{E,crit}$ and $R^*_{Q,crit}$ corresponding respectively to (i), (ii) above, and to find the corresponding $\omega^*_{E,crit}$ and $\omega^*_{Q,crit}$. These are shown in Table 2. In the case of the quasi-parallel growth rates the corresponding Q^*_{crit} is also given. The values $X_{m,E}$ and $X_{m,Q}$ in Table 2 are the corresponding stations of X at which the values of the R_{crit}'s were smallest for each given λ value.

The numerical methods used in the stability calculations were similar to those of Eagles & Weissman [1], so that we need not describe them again here in great detail. The integrations of the ordinary differential equations were carried out by a Runge-Kutta fourth-order procedure over 20 η-steps in [0, 1] in general, though checks were also made with 40 steps. Well tested computer routines were used to search for the eigenvalues $K(X)$, and the eigenfunction $g_0(X, \eta)$

TABLE 1

Critical values of R, ω and Q for various λ and X

		Based on energy growth rate		Based on quasi-parallel growth rate		
λ	X	$R_{E,crit}$	$\omega_{E,crit}$	$R_{Q,crit}$	$\omega_{Q,crit}$	Q_{crit}
8.0	0.2	65.77	1.403	69.35	1.2555	1.628
	0.4	60.54	1.206	–	–	–
	0.6	60.20	1.050	64.89	1.020	1.467
	0.8	64.17	0.930	–	–	–
9.0	0.2	55.98	1.466	59.43	1.294	1.661
	0.4	50.96	1.253	55.21	1.122	1.549
	0.6	49.87	1.087	54.90	0.993	1.455
	0.8	51.90	0.967	57.92	0.895	1.377
10.0	0.2	48.96	1.515	52.34	1.323	1.687
	0.4	44.21	1.287	48.25	1.147	1.574
	0.6	42.79	1.113	47.39	1.016	1.481
	0.8	43.85	0.988	49.14	0.920	1.405
11.0	0.2	43.69	1.554	47.03	1.345	1.709
	0.4	39.19	1.310	43.07	1.166	1.595
	0.6	37.61	1.127	41.90	1.033	1.501
	0.8	38.13	0.999	42.90	0.937	1.427
12.0	0.2	39.57	1.584	42.92	1.362	1.727
	0.4	35.29	1.325	39.09	1.180	1.612
	0.6	33.64	1.134	37.74	1.046	1.518
	0.8	33.84	1.002	38.24	0.950	1.445
14.0	0.75	27.71	1.022	31.65	0.988	1.488
	0.85	27.94	0.967	31.93	0.947	1.456
	0.95	28.41	0.922	32.48	0.914	1.428
16.0	0.6	23.94	1.107	27.83	1.074	1.564
	0.7	23.68	1.030	27.51	1.021	1.526
	0.8	23.69	0.968	27.49	0.977	1.492
	0.9	23.91	0.919	27.64	0.939	1.463

TABLE 2

Overall critical values of R and ω

λ	$R^*_{E,crit}$	$\omega^*_{E,crit}$	$X_{m,E}$	$R^*_{Q,crit}$	$\omega^*_{Q,crit}$	$X_{m,Q}$
8.0	59.82	1.11	0.516	–	–	–
9.0	49.83	1.11	0.570	54.61	1.04	0.518
10.0	42.78	1.11	0.615	47.35	1.04	0.566
11.0	37.54	1.09	0.650	41.90	1.04	0.596
12.0	33.50	1.08	0.678	37.71	1.02	0.640
14.0	27.70	1.04	0.722	31.61	1.01	0.696
16.0	23.65	1.00	0.745	27.48	0.99	0.762

(The last figure in columns 2, 4, 5 and 7 is subject to an uncertainty of ± 3).

was constructed. The derivatives with respect to X were determined in general by simple central difference formulae, and it was found that a step length of $\Delta X = 0.02$ was satisfactory. After use of the existence condition (3.10) the equation (3.8a) was solved for f_1 as a check, taking an independently programmed expression for the righthand side. However, the computational task here was considerably more complicated than that of Eagles & Weissman [1], partly because the steady-state solution $F(X, \eta)$ had to be calculated first and stored for each value of λ, which in itself took a considerable amount of computer time ($\simeq$ 6 ULCC CDC 7600 units for each λ value). Typically the calculations of the value of R_{crit} for a fixed λ value and for five values of X took about 9 ULCC CDC 7600 units.

Figure 4 shows the dependence on λ of our two critical Reynolds numbers $R^*_{E,crit}$ and $R^*_{Q,crit}$. One way of interpreting Figure 4 is to think of ϵ as a given small parameter, so that the channel with walls $y = 1 + \frac{1}{2}\tanh(\epsilon x)$ is fixed; and to think of the Reynolds number R as a given large parameter. Then calculate $\lambda = \epsilon R$ and examine the position of the point (R, λ) in Figure 4. If the point is to the left of the continuous curve then our stability theory predicts that all disturbances of the type considered here will decay downstream. If the point is to the right then the prediction is that some waves will grow, albeit for some limited range of X values. It would be interesting to see if such predictions agree with experimental findings and/or to know whether in practice the observation of such growing disturbances is rather difficult or not, with regard to the rather small growth rates involved and the fairly limited range of X values over which they grow at values of the Reynolds number R not too far above the critical value $R^*_{E,crit}$. Also, of course, it may be that because a physical disturbance would presumably include components of perhaps many different frequencies a clear-cut observation of the dominant mode is difficult to achieve. However there is some encouragement from the experimental

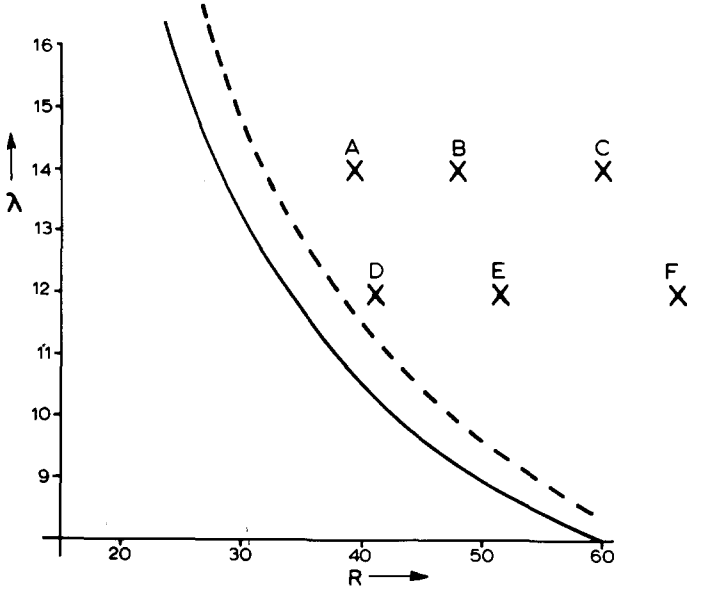

Figure 4. The dependence of the overall critical Reynolds numbers on λ. The continuous curve shows $R^*_{E,crit}$ and the dashed curve shows $R^*_{Q,crit}$, as defined in Sec. 4. Both curves pass through the point $(R, \lambda) = (3848, 0)$ which corresponds to plane Poiseuille flow.

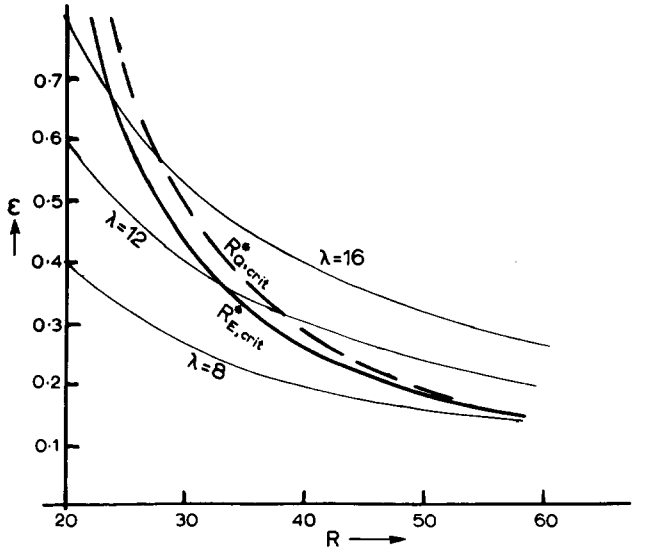

Figure 5. The dependence of the overall critical Reynolds numbers on λ. The continuous curve shows $R^*_{E,crit}$, the nonparallel flow result, and the dashed curve shows $R^*_{Q,crit}$, the quasi-parallel result. Both curves pass through the point $(R, \epsilon) = (3848, 0.0)$ of plane Poiseuille flow.

evidence on boundary layer stability that theory and observation have a close correspondence for fixed frequency disturbances (Gaster [4], Smith [5]).

It should perhaps be emphasised here that in the limit as $\epsilon \to 0$, with λ fixed and nonzero, the first approximation to the steady state flow remains completely different from a Poiseuille flow in any region of finite X values. Our calculations are based on this limit which we believe should give fairly accurate predictions at practical values of interest. Thus the critical Reynolds numbers, both the quasi-parallel and the non-parallel ones, with $\lambda \neq 0$ are expected to be less than the value $R_{crit} = 3848$ which holds for Poiseuille flow, the increased range of instability occurring mainly because of the more unstable basic velocity profiles, especially near the mouth of the channel at $X = 0$. The velocity profiles there can develop inflexion points and so would perhaps tend to be controlled more by classical inviscid, Rayleigh-type, instability features. There can be therefore a gradual qualitative adjustment from the stability properties of plane Poiseuille flows to those of inflexional profiles as the motion proceeds. On the other hand, with $\lambda = 0$ and $R \neq 0$ we have $\epsilon = 0$. The basic flow is then Poiseuille flow everywhere and the critical value of R is 3848. Both the full and the dashed curves in Figure 4 pass through the point $(R, \lambda) = (3848, 0)$, giving consistency with the results of plane Poiseuille flow. Note our R is 2/3 times the usual R often used which is based on the channel half-width and the maximum velocity when the flow is Poiseuille flow.

The computations were restricted to the range $8 \leqslant \lambda \leqslant 16$ purely because of the time-consuming nature of the work. This range was thought to give the most interesting results, however, inasmuch as the critical Reynolds numbers in this range are typically much smaller than those for Poiseuille flow. In Figure 5 we plot the stability boundaries in the R, ϵ plane. In particular the contours $\lambda = 8$, 12 and 16 are shown in this plane. The point $\epsilon = 0$, $R = 3848$ would correspond to the Poiseuille flow case. For $\epsilon = 0$, $R < 3848$ we have stable Poiseuille flow, and for $\epsilon = 0$, $R > 3848$ we have unstable Poiseuille flow.

In order to give some idea of the possible orders of magnitude of the growth of the kinetic energy of the disturbance, we may imagine an experiment in which the channel is fixed, i.e. ϵ is fixed and the Reynolds number R is gradually increased. This corresponds to the point (R, λ) in Figure 4 being moved gradually along the straight line $\lambda = \epsilon R$. Disturbances whose kinetic energy densities exhibit some growth downstream would first be possible when R is just greater than $R^*_{E,crit}$ with $\omega \simeq \omega^*_{E,crit}$, and for a small range of X around $X_{m,E}$. If we continue to increase R then the range of frequencies allowing such growing waves will increase, and the range of X for which some frequencies allow growth will increase. A detailed calculation of these possibilities is feasible in principle although of course it would be another major computational task. Instead of attempting this, we have chosen certain values of ϵ and have chosen $\omega = \omega^*_{E,crit}$ for each of these values of ϵ. We have then considered a fixed value of R above $R^*_{E,crit}$ and calculated the growth rate $G_E(X)$ over a range of X stations.

In figure 6 we present graphs of some of these growth rates against X. Calculations of the growth of the kinetic energy density $E(X)$ were also made and are presented in Table 3. We see

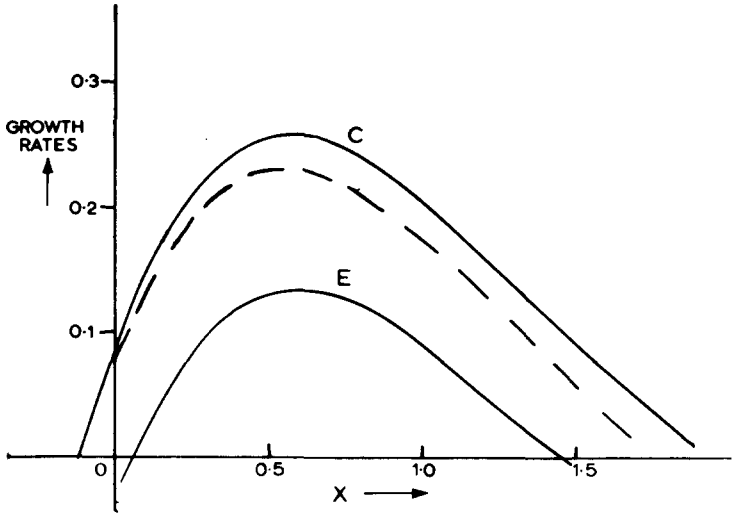

Figure 6. The growth rate $G_E(X)$ of the kinetic energy density of the disturbance for the points E and C shown previously on figure 4, with the values of $\omega = \omega^*_{E,crit}$ from Table 3. The dashed curve shows the values of $-2Q_i(X)$ for point C, i.e. the corresponding quasi-parallel growth rate.

TABLE 3

Relative growth of the kinetic energy density E(X). Here $\omega^*_{E,crit}$ is the critical ω for the appropriate ϵ, and $R^*_{E,crit}$ is the corresponding critical Reynolds number. X_0 and X_1 are the limits of the range of X for which the corresponding E(X) is growing downstream.

Point in Figure 4	ϵ	$\omega^*_{E,crit}$	$R^*_{E,crit}$	$R/R^*_{E,crit}$	Relative Growth	X_0	X_1
A	0.358	1.08	33.5	1.17	35%	0.16	1.56
D	0.293	1.09	37.5	1.09	15%	0.24	$\simeq$ 1.1
B	0.293	1.09	37.5	1.27	100%	0.01	$\simeq$ 1.80
E	0.234	1.11	42.8	1.20	60%	0.06	1.46
C	0.234	1.11	42.8	1.40	285%	−0.12	$\simeq$ 1.94
F	0.181	1.11	49.8	1.33	235%	−0.08	1.65

that the greatest relative growth found in these calculations is about 285% for a value of R about 40% above the critical R value for that particular channel. In calculating these figures we used the expression

$$E(X) = \exp\left\{\int^{X} G_E(X)dX/\epsilon\right\}. \tag{4.1}$$

If we had used the perhaps more natural expression

$$\hat{E}(X) = \sqrt{E(X)},$$

then the corresponding growth rates would have been halved, and the relative growths of $E(X)$ considerably smaller. This might tend to suggest that there would probably be no clear-cut distinction experimentally between the 'stable' and 'unstable' regions in Figure 4. For when the Reynolds number R is just greater than its critical value the disturbances can grow so little, over such a limited range of X stations, that observations of random or fixed frequency disturbances could well be extremely difficult experimentally. It might be suggested therefore that the Reynolds number would have to be considerably above critical for disturbance growths to be appreciable in practice. Whether or not such suggestions do prove well-founded in practice remains to be seen. For, alternatively, it could be that because of the long length scale $[O(R)]$ associated with the dependence on X the growths predicted from our work are indeed observable.

5. Further discussion

For the particular class of channels whose walls are described by $y = (1 + \frac{1}{2}\tanh \epsilon x)$ we have calculated the critical Reynolds number below which all fixed frequency waves have their kinetic energy density $E(X)$ decaying with distance downstream. This main result is illustrated in Figure 4. For values of the Reynolds number R greater than the above critical value the results show that some of the waves will have growing kinetic energy density as we move downstream, for some limited range of stations X. The results of this calculation, with the non-parallelism of the basic flow taken into account, give critical Reynolds numbers of the order of 10% below those of the quasi-parallel theory, as Figure 4 shows.

The testing of the relevance of our results to the stability of the real fluid flow is not necessarily a clear-cut affair, of course, since unless the Reynolds number R is very much larger than the critical value the disturbances will simply not grow considerably, at least according to our nonparallel linear theory. However, there are nevertheless some grounds for reasonable optimism regarding experimental comparisons. The relevant theoretical results here are shown in Table 3. If it is assumed, by way of fourier decomposition, that random disturbances to the steady flow may be represented by components of the type of fixed frequency waves considered in this paper, then the theory predicts that there is a limited range of values of X over which the steady basic flow might be expected to show some disturbance growth. This is a different situation from that of the main nonparallel flows to have been studied previously

using nonparallel stability theory, the straight-walled channel and the boundary layer flows, for in those two cases, where there is a simple basic flow, growing disturbances would be expected to occur at all X stations for Reynolds numbers greater than a certain value. Naturally this qualitative property of our flow situation follows from quasi-parallel theory in any case since we have plane Poiseuille flow far upstream and far downstream and more unstable-looking velocity profiles in between. Nevertheless it is perhaps rather surprising that even for the relatively large values of the parameter ϵ used here (values as large as $\epsilon \simeq 0.7$) the differences between the quasi-parallel and the nonparallel critical Reynolds numbers are so small, being only about 15% at the greatest.

REFERENCES

[1] P. M. Eagles and M. A. Weissman, On the stability of slowly varying flow: the divergent channel, *J. Fluid Mech.* 69 (1975) 241-262.
[2] M. Bouthier, Stabilité linéaire des écoulements presque parallèles, I, *J. de Mécanique* 11 (1972) 1-23.
[3] M. Bouthier, Stabilité linéaire des écoulements presque parallèles, II, La couche limite de Blasius, *J. de Mécanique* 12 (1973) 75-95.
[4] M. Gaster, On the effects of boundary-layer growth on flow stability, *J. Fluid Mech.* 66 (1974) 465-480.
[5] F. T. Smith, On the non-parallel flow stability of the Blasius boundary layer, *Proc. Roy. Soc.* A 366 (1979) 91-109.
[6] C.-H. Ling and W. C. Reynolds, Non-parallel flow corrections for the stability of shear flows, *J. Fluid Mech.* 59 (1973) 571-591.
[7] P. G. Drazin, On a model of instability of a slowly-varying flow, *Quart. J. Mech. Appl. Math.* 27 (1974) 69-86.
[8] A. H. Nayfeh, D. T. Mook and W. S. Saric, Stability of non-parallel flows, *Arch. Mech. Stosow* 26 (1974) 401-406.
[9] C. B. Schubauer and H. K. Skramstad, Laminar boundary layer oscillations and transition on a flat plate, *J. Res. Nat'l Bur. Stand.* 38 (1947) 251-283.
[10] J. A. Ross, F. H. Barnes, J. G. Burns and M. A. S. Ross, The flat plate boundary layer, Part 3, Comparison of theory with experiment, *J. Fluid Mech.* 43 (1970) 819-832.
[11] L. E. Fraenkel, Laminar flow in symmetrical channels with slightly curved walls. I. On the Jeffery-Hamel solutions for flow between plane walls, *Proc. Roy Soc.* A 267 (1962) 119-138.
[12] L. E. Fraenkel, Laminar flow in symmetrical channels with slightly curved walls, II. An asymptotic series for the stream function, *Proc. Roy. Soc.* A 272 (1963) 406-428.
[13] S. Wilson, The development of Poiseuille flow, *J. Fluid Mech.* 38 (1969) 793-806.
[14] O. Tutty, *Ph.D. Thesis*, University of London, in preparation.
[15] F. T. Smith, Flow through constricted or dilated pipes and channels, Part 1, *Quart. J. Mech. Appl. Math.* 29 (1976) 343-364.
[16] F. T. Smith, Flow through constricted or dilated pipes and channels, Part 2, *Quart. J. Mech. Appl. Math.* 29 (1976) 365-376.
[17] F. T. Smith, The separating flow through a severely constricted symmetric tube, *J. Fluid Mech.* 90 (1979) 725-754.
[18] S. Goldstein, On laminar boundary layer flow near a point of separation, *Quart. J. Mech. Appl. Math.* 1 (1948) 43-69.
[19] H. B. Keller and T. Cebeci, Accurate numerical methods for boundary layer flows 1. Two-dimensional laminar flows, *2nd Int. Conf. on Num. Meth. in Fluid Dynamics*, Berkeley, Springer publications, 92-105.
[20] F. T. Smith, Boundary layer flow near a discontinuity in wall conditions, *J. Inst. Maths. & Its Applics.* 13 (1974) 127-145.
[21] M. Allmen, *Ph.D. Thesis*, City University, London, in preparation.
[22] J. T. Stuart, On the nonlinear mechanics of wave disturbances in stable and unstable parallel flows. Part 1, The basic behaviour in plane Poiseuille flow, *J. Fluid Mech.* 9 (1960) 353-370.
[23] J. Watson, On the nonlinear mechanics of wave disturbances in stable and unstable parallel flows, Part 2. The development of a solution for plane Poiseuille flow and for plane Couette flow, *J. Fluid Mech.* 9 (1960) 371-389.